

## A Modular Framework to Generate Robust Biped Locomotion: From Planning to Control

Mohammadreza Kasaei · Ali Ahmadi · Nuno Lau · Artur Pereira

Received: date / Accepted: date

**Abstract** Biped robots are inherently unstable because of their complex kinematics as well as dynamics. Despite the many research efforts in developing biped locomotion, the performance of biped locomotion is still far from the expectations. This paper proposes a model-based framework to generate stable biped locomotion. The core of this framework is an abstract dynamics model which is composed of three masses to consider the dynamics of stance leg, torso and swing leg for minimizing the tracking problems. According to this dynamics model, we propose a modular walking reference trajectories planner which takes into account obstacles to plan all the references. Moreover, this dynamics model is used to formulate the controller as a Model Predictive Control (MPC) scheme which can consider some constraints in the states of the system, inputs, outputs and also mixed input-output. The performance and the robustness of the proposed framework are validated by performing several numerical simulations using MATLAB. Moreover, the framework is deployed on a simulated torque controlled humanoid to verify its performance and robustness. The simulation results show that the proposed framework is capable of generating biped locomotion robustly.

**Keywords** Robust biped locomotion · Model Predictive Control (MPC) · Accurate dynamics model · Humanoid robots.

---

Mohammadreza Kasaei, Nuno Lau, Artur Pereira  
IEETA / DETI University of Aveiro 3810-193 Aveiro, Portugal  
Tel.: +351-234-370-500  
Fax: +351-234-370-545  
E-mail: {Mohammadreza, nunolau, artur}@ua.pt

Ali Ahmadi  
E-mail: Ahmadi.bps@gmail.com

## 1 Introduction

Humanoid robots have been expected to be adapted in our real environment for helping us to perform our daily-life tasks. Developing a robust walking framework for humanoid robots has been researched for decades and it is still a challenging problem in the robotics community. The complexity of this problem derives from several different aspects like considering an accurate hybrid dynamics model, designing and developing an appropriate controller based on the dynamics model. Additionally, the robot's hardware should be capable enough to follow the output of the controller precisely.

The wide range of applications of these robots motivates researchers to tackle this complex problem. Research in this field can be classified into two main classes: model-free and model-based [14]. The model-free approaches try to generate walking patterns by generating rhythmic patterns for each limb and without caring about the dynamics model of the system. Unlike model-free approaches, the fundamental core of the model-based approaches is a dynamics model of the robot which is used to describe the overall behavior of the system in an abstract manner. The main focus of this paper is on a model-based approach.

The first question in designing a model-based walking is *how accurate should the model be?*. To answer this question, two points of view exist: (i) using a whole-body dynamics model (true model), (ii) using an abstract model. We believe that for designing a dynamics model of a system, a trade-off between accuracy and simplicity should be taken into account. Although the whole body dynamics model is more accurate than an abstract model, it is nonlinear and computationally demanding. Thus, it demands a high computational effort and also it is platform-dependent.

Linear Inverted Pendulum Model (LIPM) is one of the common dynamics models in the literature [10]. The popularity of this model originates on its linearity and simplicity and also on its ability to generate a feasible, fast and efficient trajectory of the Center of Mass (COM). This model describes the dynamics of a humanoid robot just by considering a single mass that is connected to the ground via a massless rod (see Fig. 1.(a)). In this model, the single mass is assumed to move along a horizontal plane and based on this assumption, the motion equations in sagittal and frontal planes are decoupled and independent. Several studies used this model to develop an online walking generator based on optimal control [15] and also linear MPC [8, 2, 18]. Several extensions of LIPM have been proposed to increase the accuracy of this model while keeping simplicity level [21, 5, 17]. The three-mass model is one of the extended versions of LIPM [23, 20, 21]. As it is shown in Fig. 1.(b), this model considers the masses of legs and the torso to increase the accuracy of the model. It should be mentioned that to keep the model linear, the vertical motions of the masses are considered to be smooth and the vertical accelerations are neglected.

In this paper, the three-mass dynamics model is used as our dynamics model and we propose a modular architecture to develop a robust walking framework. The proposed framework is composed of several basic and reusable blocks which can not only reduce the complexity of the system but also can be a key to advancements in research and development. In this framework, the problem of dynamics walking will be formulated as a linear MPC to predict the behavior of the system over a

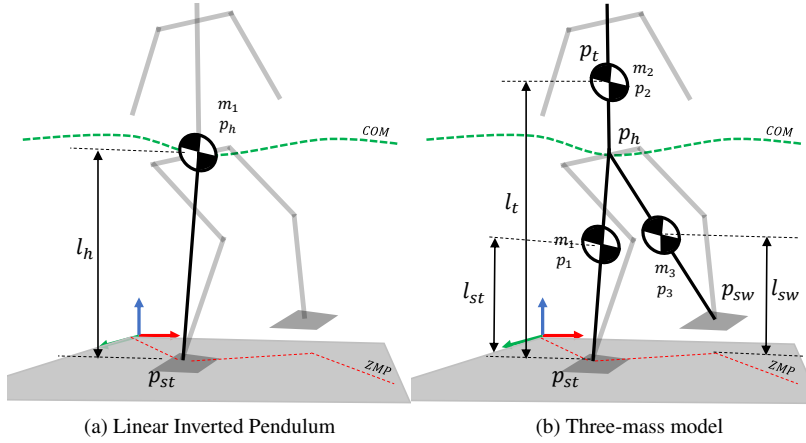


**Fig. 1** Abstract Dynamics Models: (a) represents the Linear Inverted Pendulum Model (LIPM); (b) represents three-mass model.

prediction horizon to determine the optimum control inputs. Moreover, the process of generating walking reference trajectories will be decomposed into three levels to reduce the complexity of planning. Besides, the results of several simulations will be presented to show the performance and the robustness of the proposed walking scheme.

The remainder of this paper is structured as follows: Section 2 gives an overview of related work. In Section 3, three-mass dynamics model will be reviewed briefly. Afterward, in Section 4, this dynamics model is used to design a walking controller based on MPC scheme. Section 5 gives an overview of the reference trajectories generator. In Section 6, the overall architecture of the framework will be presented. In Section 7, a set of simulation scenarios will be designed and performed to examine the tracking performance and robustness of the proposed controller. Finally, conclusions and future research are presented in Section 8.

## 2 Related Work

The main idea behind using a simplified model is fading the complexity of the control system and organizing the control system as a hierarchy. In hierarchical control approaches, a simplified dynamics model is used to abstract the overall behaviours of the system and then these behaviours will be converted to individual actuator inputs using a detailed full-body inverse dynamics [5]. In such approaches, the overall performance of the system depends on the matching between the abstract model and the exact model. Several simplified models have been proposed and those more related to our work will be reviewed in the following of this section.

Hemami and Golliday [7] proposed Inverted Pendulum (IP) which approximates the overall dynamics of a humanoid robot (during single support phase) just by a single mass that is connected to ground via a mass-less rod. This model is not only simple and physically accurate but also computationally efficient.

Kajita and Tani [12] proposed a linear version of IP by restricting the vertical motion of the mass. Based on this constraint, the mass is limited to move along a horizontal pre-defined plane. Accordingly, the dynamics system becomes a first-order linear system which provides an appropriate framework to control. Later, Kajita et al. [11] extended this model and introduced Three Dimensional Linear Inverted Pendulum Model (3D-LIPM). They explained how this model should be used to generate walking. Afterward, in [10], they used the concept of ZMP to develop a control framework based on preview control to generate stable locomotion. The performance of their framework has been validated using several simulations.

Albert and Gerth [1] extended LIPM by considering the mass of swing leg to improve gait stability and they named it Two Masses Inverted Pendulum Model (TMIPM). In their approach, swing leg and ZMP trajectories should be generated firstly and then, according to these trajectories, the trajectory of COM will be generated using a linear differential equation. They proposed an extended version of TMIPM which considers the mass of the thigh, the shank and the foot of the swinging leg and they named it Multiple Masses Inverted Pendulum Model (MMIPM). TMIPM and MMIPM are more accurate than LIPM, they need an iterative algorithm to define the COM trajectory due to dependency of motions of the masses to each other.

Shimmyo et al. [21] extended the LIPM by considering three masses to decrease the modelling error and improve the performance. In their model, the masses were located on the torso, the right leg, and the left leg. They made two assumptions to design a preview controller which were considering constant vertical position for the masses and also constant mass distribution. The performance of their approach has been validated through several experiments.

Faraji and Ijspeert [5] proposed a dynamics model which is composed of three linear pendulums to model the behaviour of stance leg, swing leg and torso dynamics and they named it 3LP. They argued that, due to the linearity of this model, it is fast and computationally similar to LIPM such that it can be used in modern control architectures from the computational perspective. The performance of their model has been proven using a set of simulations. Simulation results showed that their framework was able to generate a robust walking with wide range of speeds without requiring off-line optimizations and tuning of parameters.

Several extended version of LIPM have been proposed to consider the momentum around the COM. In [19],[17], robot's legs are considered to be massless and their motions do not have any effect in dynamics. In our previous work [13], we extended the dynamics model presented in [19] by considering the mass of stance leg and we explained how this model can be represented by a first order differential equation which can be used to design a controller to plan and track the walking reference trajectories.

In the rest of this paper, we tackle the problem of developing a robust walking by presenting a modular framework. Particularly, we will start by explaining how three-mass dynamics model can be used to formulate the walking controller as a linear MPC which is not only able to track the reference trajectories optimally even in presence of measurement noise, but also robust against disturbances. Furthermore, we will present the overall architecture of our framework and then we design a set of

simulation scenarios to validate the performance and examining the robustness of the framework.

### 3 Dynamics Model

This section will be started by a brief reviewing of the Zero Momentum Point (ZMP) concept which is one of the well-known criteria in developing stable dynamic walking. Afterward, the ZMP concept will be used to define the overall dynamics of a biped robot as a state-space system.

#### 3.1 Zero Momentum Point and Gait Stability

Several criteria have been introduced to analyze the stability of a biped robot. ZMP has been very often utilized to develop stable locomotion. In fact, ZMP is the point on the ground plane where the ground reaction force (GRF) acts to cancel the inertia and gravity [24]. Generally, the robot stability is guaranteed by keeping the ZMP inside the support polygon (the area which is specified by the convex hull of foot or feet touching the ground). For a dynamics model which is composed of  $n$  parts, ZMP can be calculated using the following equation:

$$p = \frac{\sum_{k=1}^n m_k c_k (\ddot{z}_k + g) - \sum_{k=1}^n m_k z_k \ddot{c}_k}{\sum_{k=1}^n m_k (\ddot{z}_k + g)}, \quad (1)$$

where  $g$  represents the acceleration of gravity,  $p = [p^x \ p^y]^\top$  represents the position of ZMP,  $m_k$  is the mass of each part,  $c_k = [c_k^x \ c_k^y]^\top$  and  $\ddot{c}_k$  denote the position and acceleration of each mass,  $z_k, \ddot{z}_k$  are vertical position and vertical acceleration of each mass, respectively.

#### 3.2 Three-mass Dynamics Model

Three-mass model abstracts the dynamics model of a biped robot by considering three masses. As shown in Fig. 1(b), the masses are placed at the legs and the torso of the robot. To simplify and linearize the model, each mass is restricted to move along a horizontal plane. According to this assumption, the ZMP equations are independent and equivalent in frontal and sagittal planes. Thus, in the remaining of this paper, just the equations in the sagittal plane will be considered. Based on (1), a state-space

system can be defined to analyze the behavior of the system:

$$\frac{d}{dt} \underbrace{\begin{bmatrix} \dot{c}_1^x \\ \dot{c}_1^x \\ \ddot{c}_1^x \\ \dot{c}_2^x \\ \dot{c}_2^x \\ \ddot{c}_2^x \\ \dot{c}_3^x \\ \dot{c}_3^x \\ \ddot{c}_3^x \end{bmatrix}}_X = \underbrace{\begin{bmatrix} 0 & 1 & 0 & 0 & 0 & 0 & 0 & 0 \\ 0 & 0 & 1 & 0 & 0 & 0 & 0 & 0 \\ 0 & 0 & 0 & 0 & 0 & 0 & 0 & 0 \\ 0 & 0 & 0 & 0 & 1 & 0 & 0 & 0 \\ 0 & 0 & 0 & 0 & 0 & 1 & 0 & 0 \\ 0 & 0 & 0 & 0 & 0 & 0 & 0 & 0 \\ 0 & 0 & 0 & 0 & 0 & 0 & 0 & 1 \\ 0 & 0 & 0 & 0 & 0 & 0 & 0 & 0 \\ 0 & 0 & 0 & 0 & 0 & 0 & 0 & 0 \end{bmatrix}}_A \underbrace{\begin{bmatrix} \dot{c}_1^x \\ \dot{c}_1^x \\ \ddot{c}_1^x \\ \dot{c}_2^x \\ \dot{c}_2^x \\ \ddot{c}_2^x \\ \dot{c}_3^x \\ \dot{c}_3^x \\ \ddot{c}_3^x \end{bmatrix}}_X + \underbrace{\begin{bmatrix} 0 & 0 & 0 \\ 0 & 0 & 0 \\ 1 & 0 & 0 \\ 0 & 0 & 0 \\ 0 & 1 & 0 \\ 0 & 0 & 0 \\ 0 & 0 & 0 \\ 0 & 0 & 0 \\ 0 & 0 & 1 \end{bmatrix}}_B \underbrace{\begin{bmatrix} \ddot{c}_1^x \\ \ddot{c}_2^x \\ \ddot{c}_3^x \end{bmatrix}}_U \quad (2)$$

$$y = \underbrace{\begin{bmatrix} 1 & 0 & 0 & 0 & 0 & 0 & 0 & 0 & 0 \\ 0 & 0 & 0 & 0 & 0 & 0 & 1 & 0 & 0 \\ \frac{m_1}{M} & 0 & \frac{-m_1 z_1}{Mg} & \frac{m_2}{M} & 0 & \frac{-m_2 z_2}{Mg} & \frac{m_3}{M} & 0 & \frac{-m_3 z_3}{Mg} \end{bmatrix}}_C \underbrace{\begin{bmatrix} \dot{c}_1^x \\ \dot{c}_1^x \\ \ddot{c}_1^x \\ \dot{c}_2^x \\ \dot{c}_2^x \\ \ddot{c}_2^x \\ \dot{c}_3^x \\ \dot{c}_3^x \\ \ddot{c}_3^x \end{bmatrix}}_X,$$

where  $\ddot{c}_1^x, \ddot{c}_2^x, \ddot{c}_3^x$  are the control inputs in jerk dimension,  $M$  is weight of the robot,  $m_1, m_2, m_3$  represent the mass of stance leg, torso and swing leg, respectively. Based on the output equation (y), the positions of stance leg, swing leg and also ZMP are measured at each control cycle. In the next section, the defined system will be discretized to discrete-time implementation and we will explain what type of walking objectives and constraints should be considered to generate stable dynamic walking.

#### 4 Online Walking Controller Based on MPC

In this section, the problem of the online walking controller is formulated as a linear MPC which is not only robust against uncertainties but also able to consider some constraints in the states, inputs and outputs. To do that, firstly, the presented continuous system (2) should be discretized for implementation in discrete time. Afterward, the walking objective will be formulated as a set of quadratic functions and finally walking constraints will be formulated as linear functions of the states, inputs and outputs.

##### 4.1 Discrete Dynamics Model

To discretize the system, we assume that  $\ddot{c}_1, \ddot{c}_2, \ddot{c}_3$  are linear and, based on this assumption,  $\ddot{c}_1, \ddot{c}_2, \ddot{c}_3$  are constant within a control cycle. Thus, the discretized sys-

tem can be represented as follows:

$$\begin{aligned} X(k+1) &= A_d X(k) + B_d u(k) \\ y(k) &= C_d X(k) \end{aligned} \quad (3)$$

where  $k$  represents the current sampling instance,  $A_d, B_d, C_d$  are the discretized version of the  $A, B, C$  matrices in (2), respectively. Based on this system, the state vector  $X(k)$  can be estimated at each control cycle. Thus, according to the estimated states, some objectives and constraints, the problem of determining the control inputs can be formulated as an optimization problem (a quadratic program (QP)) at each control cycle. The optimization solution specifies the control inputs which are used until the next control cycle. This optimization just considers the current timeslot, to take into account the future timeslots, a finite time-horizon is considered for the optimization process, but only the current timeslot will be applied and for each timeslot this optimization will be repeated again. Indeed, the optimization solution determines  $N_c$  (control horizon) future moves ( $\Delta U = [\Delta u(k), \Delta u(k+1), \dots, \Delta u(k+N_c-1)]^T$ ) based on the future behavior of the system ( $Y = [y(k+1|k), y(k+2|k), \dots, y(k+N_p|k)]^T$ ) over a prediction horizon of  $N_p$ .

#### 4.2 Walking Objective

Walking is periodic locomotion which can be decomposed into two main phases: *single support* and *double support*. In the double support phase, the robot tries to shift its COM to the stance foot and during single support its swing leg moves towards the next step position. In order to develop stable locomotion, robot should be able to track a set of reference trajectories while keeping its stability. As mentioned before, a popular approach to guarantee the stability of the robot is keeping the ZMP within the support polygon. According to (2), the position of the stance leg, swing leg and ZMP are measured at each control cycle. Thus, the following objectives should be considered to keep the outputs at or near the references:

$$\begin{aligned} d_1 &= \|p_z - r_z\|^2 \\ d_2 &= \|p_{st} - r_{st}\|^2 \\ d_3 &= \|p_{sw} - r_{sw}\|^2, \end{aligned} \quad (4)$$

where  $p_z, r_z, p_{st}, r_{st}, p_{sw}, r_{sw}$  are the measured and reference ZMP, and the measure and reference positions of the stance and swing legs, respectively. Moreover, to generate a smooth trajectories which are compatible with the robot structure, the control inputs are considered into the objectives for smoothing all the motions:

$$\begin{aligned} d_4 &= \|\ddot{c}_1^x\|^2 \\ d_5 &= \|\ddot{c}_2^x\|^2 \\ d_6 &= \|\ddot{c}_3^x\|^2. \end{aligned} \quad (5)$$

According to the explained objective terms, the following cost function is defined to find an optimal set of control inputs:

$$J(z_k) = \sum_{i=1}^{N_p} \sum_{j=1}^6 \alpha_j d_j(z_k) \quad (6)$$

where  $k$  is the current control interval,  $z_k^\top = \{\Delta u(k|k)^\top \ \Delta u(k+1|k)^\top \dots \Delta u(k+N_p-1|k)^\top\}$  is the QP decision and  $\alpha_j$  represents a positive gain that is assigned to each objective.

#### 4.3 Time-Varying Constraints

To ensure the feasibility of the solution that is found by the MPC, a set of constraints should be considered to avoid generating infeasible solutions. For instance, the solution should be kinematically reachable by the robot and also the ZMP should be kept inside the support polygon. Generally, a set of mixed input/output constraints can be specified in the following form:

$$Eu(k+j|k) + Fy(k+j|k) \leq G + \epsilon \quad (7)$$

where  $j$  from 0 to  $N_p$ ,  $k$  is current control cycle,  $E, F, G$  are time-variant matrices where each row represents a linear constraint.  $\epsilon$  is used to specify a constraint to be soft or hard. Additionally, using this equation, the inputs and outputs can be bounded to specified limitations.

It should be noted that the constraints in the sagittal plane are similar to those in the frontal plane. In our target framework, the constraints are time-varying and they will be determined at the beginning of each walking phase. Graphical representations of the constraints are depicted in Fig. 2. Fig. 2.(a) shows that the landing position of the swing leg should be restricted in a kinematically reachable area. This area can be approximated by a rectangle which is defined as follows:

$$E = \begin{bmatrix} 0 & 0 & 0 \\ 0 & 0 & 0 \end{bmatrix}, F = \begin{bmatrix} 0 & 1 & 0 \\ 0 & -1 & 0 \end{bmatrix}, G = \begin{bmatrix} x_{max} \\ x_{min} \end{bmatrix}, \epsilon = \begin{bmatrix} 0 \\ 0 \end{bmatrix}, \quad (8)$$

where  $x_{min}, x_{max}$  are defined based on the current position of the support foot and the robot capability. In addition to these constraints, to keep the ZMP within the support polygon, the following constraints are considered:

$$E = \begin{bmatrix} 0 & 0 & 0 \\ 0 & 0 & 0 \end{bmatrix}, F = \begin{bmatrix} 0 & 0 & 1 \\ 0 & 0 & -1 \end{bmatrix}, G = \begin{bmatrix} z_{x_{max}} \\ z_{x_{min}} \end{bmatrix}, \epsilon = \begin{bmatrix} 0 \\ 0 \end{bmatrix}, \quad (9)$$

where  $z_{x_{min}}, z_{x_{max}}$  are defined based on the walking phase and the size of the foot (please look at Fig. 2. (b, c)). It should be mentioned that the feet size of the robot is considered a bit smaller (scale = 0.9) than the real feet size to prevent ZMP from being too close to the borders of support polygon.

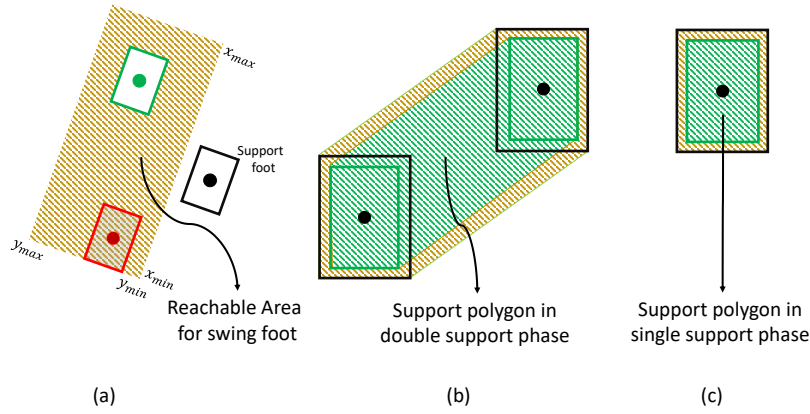


**Fig. 2** Graphical representations of the constraints: (a) kinematically reachable area for the swing leg: red rectangle represents the position of the swing leg at the beginning of step, green rectangle represents the landing location of the swing leg; (b) ZMP constraint during double support phase: green area is considered as the support polygon to avoid ZMP from being close to the borders; (c) ZMP constraint during single support phase.

## 5 Walking Reference Trajectories

According to the dynamics system presented in Section 3, three reference trajectories should be generated which are the trajectories of the feet and the ZMP. In the following of this section, we will explain how these trajectories are generated.

### 5.1 A\* Footstep Planning

Footstep planning is generally based on a graph search algorithm with a rich history [9, 6]. In our target framework, the footstep planning is composed of two stages: (i) generating a collision-free 2D body path; (ii) planning the footsteps based on the generated path. In the first stage, the environment is modeled as a 2D grid map consisting of cells that are marked as free or occupied. In this work, the size of the cell is considered to be  $0.1m^2$ , the height of obstacles is not considered and the robot can not step over an obstacle. In order to avoid collision with the obstacles, the size of the obstacles are considered to be larger than the real size (scale = 1.1). In this stage, after modeling the environment, the A\* search method is applied to find an optimum path over the free cells from the current position of the robot to the goal. Euclidean distance to the goal is used to guide the search.

In the second stage, the footsteps should be generated according to the generated path. To do so, a state variable is defined to describe the current state of the robot's feet:

$$s = (x_l, y_l, \theta_l, \phi_l, x_r, y_r, \theta_r, \phi_r) \quad (10)$$

where  $x_l, y_l, \theta_l, x_r, y_r, \theta_r$  represent the current position and orientation of the left and right feet, respectively.  $\phi_l, \phi_r$  represent the state of each foot which is 1 if the

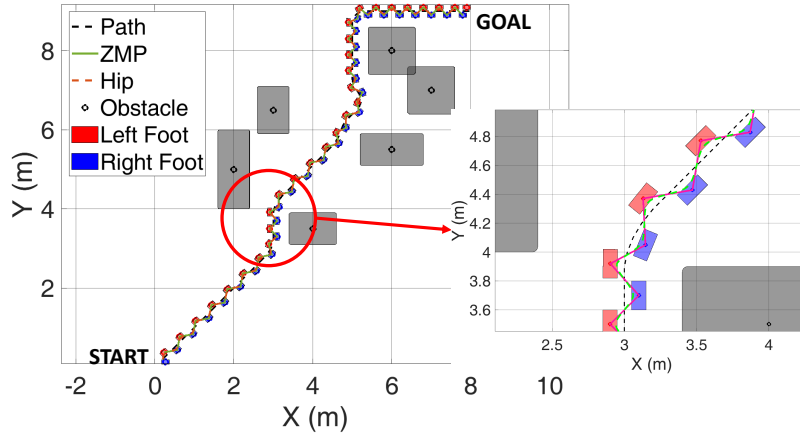


**Fig. 3** An example walking references trajectories: the gray rectangles represent the occupied cells that robot can not step; the black-dashed line represents the output of the A\* path planner; red and blue rectangles represent the footsteps which are generated based on the output of the A\*; the magenta line is the ZMP which is generated based on the outputs of the footstep planner; the lime-dashed line is the hip reference trajectory.

foot is the swing foot and  $-1$  otherwise. According to the nature of walking which is generated by moving the right and the left legs alternating, a step action is parameterized by a distance and an angle from the swing foot position at the beginning of steps  $a = (R, \sigma)$ . Based on the current state and the generated path, an action should be taken. In this paper, we consider a fix step size ( $R = 0.1$ ) and  $\sigma$  is determined by the generated path. By applying the selected action, the state transits to a new state,  $s' = t(s, a)$ . It should be noted that after each transition, the current footstep should be saved ( $f_i \quad i \in \mathbb{N}$ ) and then  $\phi_l$  and  $\phi_r$  will be toggled.

## 5.2 ZMP, Hip and Swing Reference Trajectories

Studies on human locomotion showed that while a human is walking, ZMP moves from heel to the toe during single support phase and it moves towards the COM during double support phase [3,4]. In this paper, we do not consider the ZMP movement during single support, but instead we keep it in the middle of the support foot. Thus, the ZMP reference trajectory planning can be formulated based on the generated footsteps as follows:

$$p_{st} = \begin{cases} f_i & 0 \leq t < T_{ss} \\ f_i + \frac{SL \times (t - T_{ss})}{T_{ds}} & T_{ss} \leq t < T_{ss} + T_{ds} \end{cases}, \quad (11)$$

where  $p_{st} = [p_{st}^x \quad p_{st}^y]^\top$  is the generated ZMP,  $t, T_{ss}, T_{ds}$  represent the time, duration of single and double support phases, respectively.  $SL = [SL^x \quad SL^y]$  is a vector that represents the step length and step width which are determined based on  $(R, \sigma)$ ,  $f_i = [f_i^x \quad f_i^y]$  represents the planned foot prints on a 2D surface. It should be noted that  $t$  will be reset at the end of each step ( $t \geq T_{ss} + T_{ds}$ ).

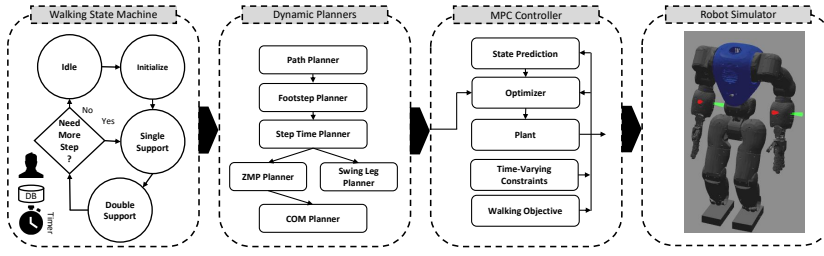


Fig. 4 Overall architecture of the proposed framework.

After generating the ZMP reference trajectory, the hip trajectory will be planned according to the generated ZMP. To do that, we assume that the COM of the robot is located at the middle the hip and, based on this assumption, the overall dynamics of the robot is firstly restricted into COM and then the reference trajectory for the hip will be generated using the analytical solution of the LIPM as follows [16]:

$$p_h(t) = p_{st} + \frac{(p_{st} - p_{h_f}) \sinh((t - t_0)\omega) + (p_{h_0} - p_{st}) \sinh((t - t_f)\omega)}{\sinh((t_0 - t_f)\omega)}, \quad (12)$$

where  $t_0$  and  $t_f$  represent the beginning and the ending times of a step and  $p_{h_0}$ ,  $p_{h_f}$  are the corresponding positions of COM at these times, respectively.

After generating the ZMP and the hip trajectory, the swing trajectory should be planned. To have a smooth trajectory during lifting and landing of the swing leg, a Bzier curve is used to generate this trajectory according to the generated footsteps and a predefined swing height.

### 5.3 Masses Reference Trajectories

The trajectories of the masses can be easily generated based on geometric relations between the generated hip, ZMP and swing leg trajectories. According to Fig.1(b), the mass of the stance leg is located in the middle of the line between the ZMP and the hip. Similarly, the mass of the swing leg is located in the middle of the line between the swing foot and the hip. To show the performance of the planners presented in this section, an example path planning scenario has been set up, which is depicted in Fig. 3. In this scenario, the robot stands at the *START* point and wants to reach to the *GOAL* point. The planning process is started by generating an optimum obstacle-free path (black-dashed line). As it is shown in Fig. 3, the generated path is far from the obstacles enough and, based on this path, the footsteps, corresponding ZMP and hip trajectories have been generated successfully.

## 6 Architecture

In this section, we used the controller and reference planner presented in the previous sections to design a robust walking framework. We explain how these modules can be

coupled together to develop a robust walking framework. According to the periodic nature of the walking, the overall process of the walking can be controlled by a state machine such that state transitions are triggered based on an associated timer and also state conditions. This state machine is composed of four main states which are depicted in Fig. 4. In the *Idle state*, the robot stands and is waiting for a start walking command. Once a walking command is received, the state transits to the *Initialize state* and the robot tries to shift its COM to the first support foot to be ready for taking the first step. In *Single Support State* and *Double Support State*, walking trajectories are generated. It should be mentioned that the associated timer will be reset at the end of the double support state. Overall architecture of the proposed framework is depicted in Fig. 4.

## 7 Simulation

In this section, a set of simulation scenarios will be designed to validate the performance and examining the robustness of the proposed framework. We firstly performed three simulations using MATLAB to evaluate the performance and robustness of the controller. Afterwards, we will deploy our framework on a simulated COMAN (a passively compliant humanoid) [22] humanoid robot to validate the performance of the proposed framework on a full size humanoid robot.

### 7.1 Simulation using MATLAB

To perform the simulations using MATLAB, a humanoid robot has been simulated according to the dynamics model presented in Section 3. The most important parameters of the simulated robot and the controller are shown in Table 1.

**Table 1** Parameters used in the simulations.

$m_1$	$m_2$	$m_3$	$l_{st}$	$l_t$	$l_{sw}$	foot width	$T_s$	$N_p$	$N_c$	$\alpha_1$	$\alpha_2$	$\alpha_3$
15kg	50kg	15kg	0.5m	1.2m	0.5m	0.1m	0.02s	80	20	20	20	20

#### 7.1.1 Tracking Performance

To check the tracking performance of the controller, the first five steps of the planned trajectories in the previous section (trajectories of the legs and the ZMP) are considered as the input references. In this simulation, the simulated robot is considered to be stopped and standing in *START* point and it should track the reference trajectories. As a result, the simulated robot walks towards the *GOAL* point while keeping its stability. The simulation results are depicted in Fig. 5. The results show that the controller is able to track the references and the ZMP is always inside the support polygon during walking. Another interesting point in the results is the trajectory of the body ( $p_t$ ). Actually, we did not determine any references for the body explicitly but it moves as we expected. As it is shown in Fig. 5.(a), it is almost near the support

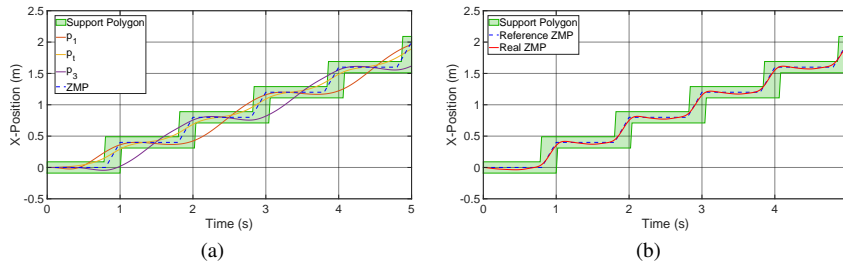


**Fig. 5** The simulation results of analyzing tracking performance: **(a)** represents the positions of the masses while walking; **(b)** represents the reference ZMP and the real ZMP.

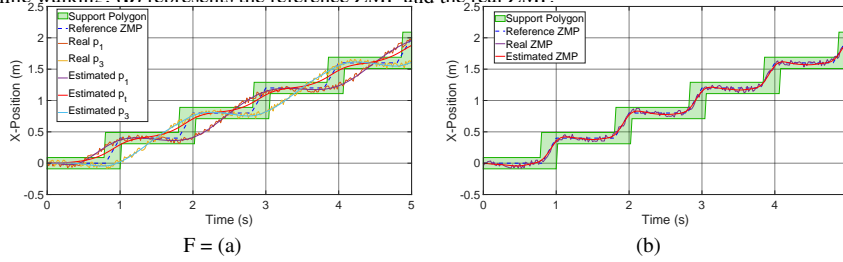


**Fig. 6** The simulation results of examining the robustness w.r.t. measurement noise: **(a)** represents the real and estimated position of the masses; **(b)** represents the real and estimated ZMP.

foot during single support phase, then by starting the double support phase, it moves towards the next support foot.

### 7.1.2 Robustness w.r.t. Measurement Noise

In the real world, measurements are always affected by noise, therefore they are never perfect. Noise can rise because of many reasons like the simplification in the modeling, discretizing and some mechanical uncertainties ( e.g. backlash of gears), etc. A robust controller should be able to estimate the correct state using the noisy measurements and minimize the effect of noise. To examine the robustness of the proposed controller regarding measurement noise, the measurements are modeled as a stochastic process by adding Gaussian noise ( $-0.05m \leq v_i \leq 0.05m \quad i = 1, 2, 3$ ) to the system output and the previous scenario has been repeated. The simulation results are shown in Fig. 6. As can be seen, the controller is robust against the measurement noise and it is able to track the references even in the presence of noise.

### 7.1.3 Robustness w.r.t. External Disturbance

A robust controller should be able to reject an unwanted external disturbance that can occur in some situations like when a robot hits an obstacle or when it has been pushed by someone. In such situations, the controller cancels the effect of the impact and tries to keep ZMP inside the support polygon by applying compensating torques. To examine the robustness of the controller w.r.t. external disturbances, an unpredictable external force is applied to the body of the robot while it is performing the previous scenario. The impact has been applied at  $t = 1.6s$  and the impact duration is  $\Delta t =$

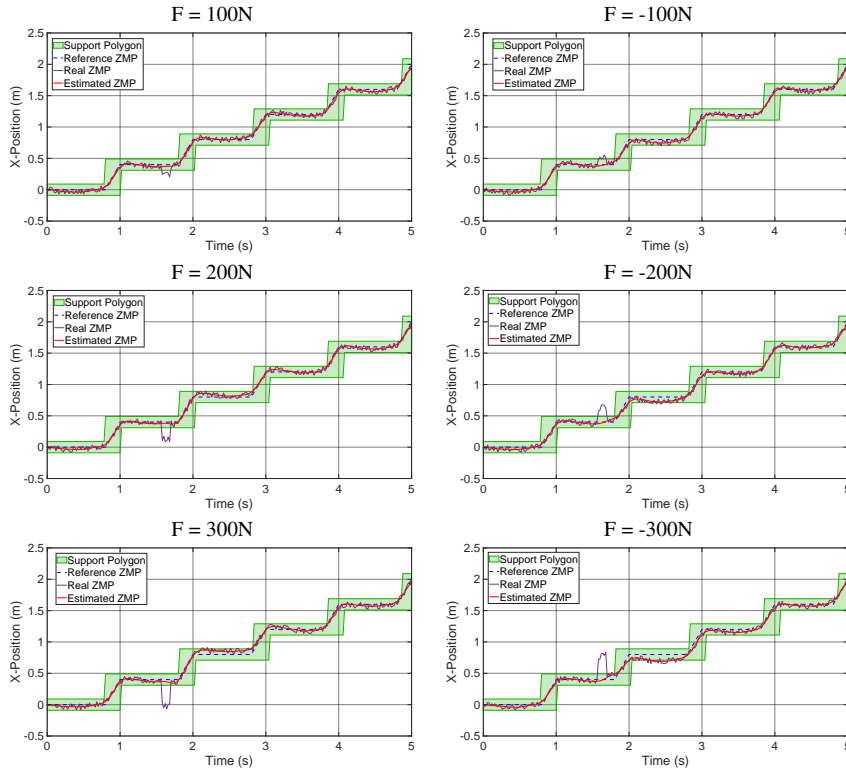


**Fig. 7** The simulation results of examining the robustness w.r.t. external disturbance: each plot represents a single simulation result.

10ms. This simulation was repeated six times with different amplitudes ( $-300N \leq F \leq 300N$ ). Moreover, to have realistic simulations, measurements are confounded by measurement noise ( $-0.05m \leq v_i \leq 0.05m \quad i = 1, 2, 3$ ). The simulation results are shown in Fig. 7. Each plot represents the result of a single simulation. As these plots show, after applying an external force, the real ZMP goes out of the support polygon quickly but the controller regains it back and keeps the stability of the robot. We increase the amplitude of the impact to find the maximum withstanding of the controller. After performing these simulations,  $F = 435N$  and  $F = -395N$  were the maximum levels of withstanding of the controller. According to the simulation results, the proposed controller is robust against external disturbance.

#### 7.1.4 Overall Performance

In order to check the overall performance of the proposed planning and controller, a path planning scenario has been designed. In this scenario, the simulated robot should walk from *START* point towards *GOAL* point. The simulation results are shown in Fig. 9. The results showed that the planner was able to generate walking reference trajectories and the controller was able to track the generated references success-

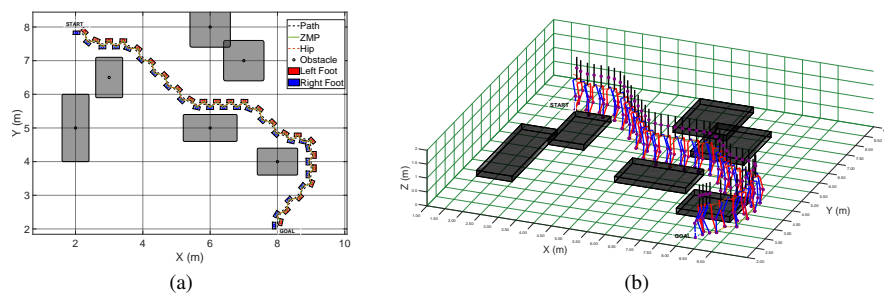


**Fig. 9** The simulation results of examining the overall performance of the proposed planner and controller. (a) represents the output of the planner; (b) represents the 3D visualization of the simulation.

fully. A video of this simulation is available online at:

<https://www.dropbox.com/s/oevqcxkyvwfad07/ICARSC2020.mp4?dl=1>.

## 7.2 Simulation using COMAN

To show the performance of our framework to control a full humanoid robot, we performed a set of simulations using a simulated COMAN humanoid in Gazebo environment which is an open-source simulation environment developed by the Open Source Robotics Foundation (OSRF). The simulated robot is 95cm tall, weighs 31kg, and has 23 DOF (6 per leg, 4 per arm and 3 between the hip and the torso). This robot is equipped with usual joint position and velocity sensors, an IMU on its hip and torque/-force sensors at its ankles.

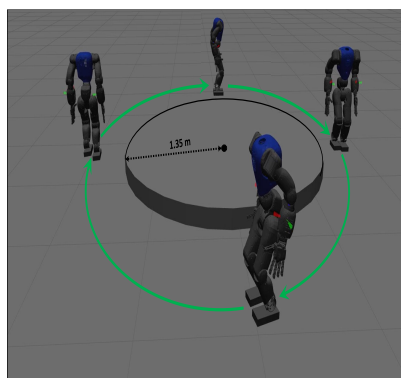


**Fig. 8** Walking around a disk: the simulated robot should follow the input command to walk around the disk.

### 7.2.1 Walking Around a Disk

This simulation is focused on testing the performance of the framework for combining turning and forward walking. In this simulation, the robot initially stays next to a large disk of radius  $1.35m$  and waiting to receive a start signal. Once the signal is generated, the robot should walk around the disk and return back to initial point. The sequences of the experiment are shown in Fig. 8. The result showed that the framework is able to combine steering and forward walking command. A video of this simulation is available online at: <https://www.dropbox.com/s/u016oup96iuz3rf/WalkingAroundADisk.mp4?dl=0>.

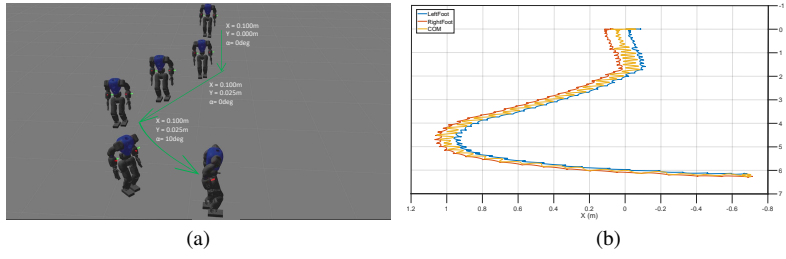


**Fig. 10** Omnidirectional walking scenario: (a) An overview of the omnidirectional walking scenario; (b) The feet and COM in the XY plane.

### 7.2.2 Omnidirectional Walking

This scenario is focused on validating the performance of the proposed framework for providing an omnidirectional walking. In this scenario, the simulated robot should track specified setpoints including step length ( $X$ ), step width ( $Y$ ) and step angle ( $\alpha$ ). At the beginning of the simulation, all the setpoints are zero and the robot is walking in place. At  $t = 8s$ , the robot is commanded to walk forward ( $X = 0.1m, Y = 0.0m, \alpha = 0.0deg/s$ ), At  $t = 24s$ , the robot is commanded to walk diagonally ( $X = 0.10m, Y = 0.025m, \alpha = 0.0deg/s$ ), at  $t = 42$ , while it is performing diagonal walking, it is commanded to turn left simultaneously ( $X = 0.1m, Y = 0.025m, \alpha = 10deg/s$ ). An overview of this scenario is depicted in Fig. 10(a). During this simulation, the position of the feet and COM has been recorded to examine the behaviour of the COM while walking and it is depicted in Fig. 10(b). According to the recorded data, the COM tends to the support foot during single support phase and moves to the next support foot during double support phase. It should be mentioned that we used a first-order lag filter to update the new setpoints to have a smooth updating. The results show that the framework is able to provide omnidirectional walking. A video of this simulation is available online at: <https://www.dropbox.com/s/604xmpjsqwnleri/OmnidirectionalWalking.mp4?dl=0>.

### 7.2.3 External Disturbance

The goal of this simulation is to evaluate the framework in terms of disturbance rejection. In this scenario, while the robot is walking in place, an impulsive external disturbance is applied to its hip and the robot should reject the disturbance to keep its stability. This simulation has been repeated with different amplitude of impact to validate the robustness of the framework and to characterize the maximum level of withstanding of the robot. The amplitude of the first impact is  $500N$  and it has been increased

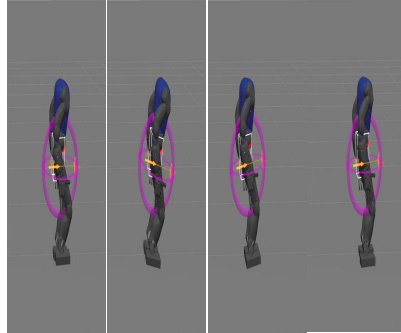


**Fig. 11** A set of snapshots of external disturbance rejection scenario. The simulated robot is subject to a  $2000N$  forward push applied on its hip.

until the robot could not regain its stability and fell. Fig. 11 shows an snapshot of the simulation while the robot is subject to a severe push ( $2000N$ ). Fig. 11 shows that the robot could reject this disturbance and regain its stability. The simulation results show the framework is robust against external disturbances and  $F = 2500N$  were the maximum levels of withstanding of the robot. A video of this simulation is available online at: <https://www.dropbox.com/s/k6lrdit222vzbz56/PushRecovery1.mp4?dl=0>.

## 8 Conclusion

In this paper, we have developed a model-based walking framework to generate robust biped locomotion. The core of this framework is a dynamics model that abstracts the overall dynamics of a robot into three masses. In particular, this dynamics model and the ZMP concept were used to represent the overall dynamics model of a humanoid robot as a state-space system. Then, this state-space system was used to formulate the walking controller as a linear MPC which generates the control solution using an online optimization subject to a set of objectives and constraints. Later, we have presented a hierarchical planning approach which was composed of three main levels to generate walking reference trajectories. To examine the performance of the proposed planner, a path planning simulation scenario has been designed to validate the performance of the planner. Afterward, according to the planned reference trajectories, a set of numerical simulations has been performed using MATLAB to examine the performance and robustness of the controller. Besides, the proposed framework has been deployed on a simulated COMAN humanoid robot to conduct a set of simulations using an ODE based simulator environment. The simulation results validated the performance and robustness of the proposed framework. In future work, we would like to extend this work to investigate the effect of online modification of step position and duration.

## Acknowledgment

This research is supported by Portuguese National Funds through Foundation for Science and Technology (FCT) through FCT scholarship SFRH/BD/118438/2016 and also in the context of the project UIDB/00127/2020.

## References

1. Albert, A., Gerth, W.: Analytic path planning algorithms for bipedal robots without a trunk. *Journal of Intelligent and Robotic Systems* **36**(2), 109–127 (2003)
2. Brasseur, C., Sherikov, A., Collette, C., Dimitrov, D., Wieber, P.B.: A robust linear MPC approach to online generation of 3d biped walking motion. In: 2015 IEEE-RAS 15th International Conference on Humanoid Robots (Humanoids), pp. 595–601. IEEE (2015)
3. Dasgupta, A., Nakamura, Y.: Making feasible walking motion of humanoid robots from human motion capture data. In: Proceedings 1999 IEEE International Conference on Robotics and Automation (Cat. No. 99CH36288C), vol. 2, pp. 1044–1049. IEEE (1999)

4. Erbacher, K., Okazaki, A., Obiya, K., Takahashi, T., Kawamura, A.: A study on the zero moment point measurement for biped walking robots. In: 7th International Workshop on Advanced Motion Control. Proceedings (Cat. No. 02TH8623), pp. 431–436. IEEE (2002)
5. Faraji, S., Ijspeert, A.J.: 3lp: A linear 3d-walking model including torso and swing dynamics. *the international journal of robotics research* **36**(4), 436–455 (2017)
6. Griffin, R.J., Wiedebach, G., McCrory, S., Bertrand, S., Lee, I., Pratt, J.: Footstep planning for autonomous walking over rough terrain. arXiv preprint arXiv:1907.08673 (2019)
7. Hemami, H., Golliday Jr, C.: The inverted pendulum and biped stability. *Mathematical Biosciences* **34**(1-2), 95–110 (1977)
8. Herdt, A., Perrin, N., Wieber, P.B.: Walking without thinking about it. In: Intelligent Robots and Systems (IROS), 2010 IEEE/RSJ International Conference on, pp. 190–195. IEEE (2010)
9. Hornung, A., Bennewitz, M.: Adaptive level-of-detail planning for efficient humanoid navigation. In: 2012 IEEE International Conference on Robotics and Automation, pp. 997–1002. IEEE (2012)
10. Kajita, S., Kanehiro, F., Kaneko, K., Fujiwara, K., Harada, K., Yokoi, K., Hirukawa, H.: Biped walking pattern generation by using preview control of zero-moment point. In: Robotics and Automation, 2003. Proceedings. ICRA'03. IEEE International Conference on, vol. 2, pp. 1620–1626. IEEE (2003)
11. Kajita, S., Matsumoto, O., Saigo, M.: Real-time 3D walking pattern generation for a biped robot with telescopic legs. In: Robotics and Automation, 2001. Proceedings 2001 ICRA. IEEE International Conference on, vol. 3, pp. 2299–2306. IEEE (2001)
12. Kajita, S., Tani, K.: Study of dynamic biped locomotion on rugged terrain-derivation and application of the linear inverted pendulum mode. In: Robotics and Automation, 1991. Proceedings., 1991 IEEE International Conference on, pp. 1405–1411. IEEE (1991)
13. Kasaei, M., Lau, N., Pereira, A.: An optimal closed-loop framework to develop stable walking for humanoid robot. In: Autonomous Robot Systems and Competitions (ICARSC), 2018 IEEE International Conference on, pp. 30–35. IEEE (2018)
14. Kasaei, M., Lau, N., Pereira, A.: A fast and stable omnidirectional walking engine for the nao humanoid robot. In: Robot World Cup, pp. 99–111. Springer (2019)
15. Kasaei, M., Lau, N., Pereira, A.: A robust biped locomotion based on linear-quadratic-gaussian controller and divergent component of motion. In: 2019 IEEE/RSJ International Conference on Intelligent Robots and Systems, pp. 1429–1434. IEEE (2019)
16. Kasaei, M.M., Lau, N., Pereira, A.: A model-based biped walking controller based on divergent component of motion. In: 2019 IEEE International Conference on Autonomous Robot Systems and Competitions (ICARSC), pp. 1–6. IEEE (2019)
17. Kasaei, S.M., Lau, N., Pereira, A.: A reliable hierarchical omnidirectional walking engine for a bipedal robot by using the enhanced lip plus flywheel. In: Human-centric Robotics-Proceedings Of The 20th International Conference Clawar 2017, p. 399. World Scientific (2017)
18. Mirjalili, R., Yousefi-Korna, A., Shirazi, F.A., Nikkhah, A., Nazemi, F., Khadiv, M.: A whole-body model predictive control scheme including external contact forces and COM height variations. In: 2018 IEEE-RAS 18th International Conference on Humanoid Robots (Humanoids), pp. 1–6. IEEE (2018)
19. Pratt, J., Carff, J., Drakunov, S., Goswami, A.: Capture point: A step toward humanoid push recovery. In: 2006 6th IEEE-RAS international conference on humanoid robots, pp. 200–207. IEEE (2006)
20. Sato, T., Sakaino, S., Ohnishi, K.: Real-time walking trajectory generation method with three-mass models at constant body height for three-dimensional biped robots. *IEEE transactions on industrial electronics* **58**(2), 376–383 (2010)
21. Shimmyo, S., Sato, T., Ohnishi, K.: Biped walking pattern generation by using preview control based on three-mass model. *Industrial Electronics, IEEE Transactions on* **60**(11), 5137–5147 (2013)
22. Spyrakos-Papastavridis, E., Medrano-Cerda, G.A., Tsagarakis, N.G., Dai, J.S., Caldwell, D.G.: A push recovery strategy for a passively compliant humanoid robot using decentralized lqr controllers. In: 2013 IEEE International Conference on Mechatronics (ICM), pp. 464–470. IEEE (2013)
23. Takenaka, T., Matsumoto, T., Yoshiike, T.: Real time motion generation and control for biped robot-1st report: Walking gait pattern generation. In: Intelligent Robots and Systems, 2009. IROS 2009. IEEE/RSJ International Conference on, pp. 1084–1091. IEEE (2009)
24. Vukobratovic, M., Frank, A., Juricic, D.: On the stability of biped locomotion. *Biomedical Engineering, IEEE Transactions on* (1), 25–36 (1970)